Irrigation's Influence on Precipitation: Texas High Plains, U.S.A

Nathan Moore and Stuart Rojstaczer

Center for Hydrologic Science, Division of Earth & Ocean Sciences, Duke University, Durham, NC

Abstract. Using bias-corrected Nexrad precipitation estimates and spatial statistics of rainfall intensity, we examine the influence of irrigation on summer precipitation in the Texas High Plains. In this region, human alteration of the surface water and energy balance has been extreme. Irrigation enhances precipitation downwind, yielding storms of greater duration, length, and accumulation. Irrigation water is not a significant source of moisture feeding precipitation; rather, the cool, wet surface increases low-level instability, triggering storms. We estimate that an additional 6% to 18% of summer precipitation attributable to irrigation falls ~90 km downwind of the irrigated region.

1. Introduction

Human modification of the landscape can significantly alter the hydrologic cycle and the land surface energy budget. Urbanization has been shown to influence local precipitation [*Lo et al*, 1997] and large-scale irrigation has been conjectured, on the basis of modeling studies, to influence local and regional precipitation [e.g., *Chen and Avissar,* 1994; *De Ridder and Gallée,* 1998*; Pielke et al.*, 1997]. However, evidence of an irrigation influence has been equivocal. Stidd [1975] suggested that irrigation induced increased precipitation in the entire area surrounding the Columbia River Basin. It is difficult to understand, however, why precipitation would be enhanced both upwind and downwind of areas of major irrigation and Fowler and Helvey [1974] found no evidence of such a relationship in this region. Barnston and Schickedanz [1984], using principal components analysis (PCA), observed precipitation patterns in monthly rainfall data (1930-1970) of the Texas High Plains that were statistically significant and spatially overlapping or nearby irrigated regions. Moore and Rojstaczer [2001] performed the same analysis for the same region over a different time period (1948 to 1997) and found no statistically significant evidence for a consistent irrigation effect in the monthly precipitation data; PCA was not sensitive enough to identify a clear signal. An equivocal pattern of precipitation *suppression*, however, was identified in some of the principal components. These results motivated more careful inspection of irrigation effects with greater spatial and temporal resolution -- the focus of this study.

Irrigation in the Texas High Plains (Plate 1) represents one of the largest human-induced hydrologic disturbances in North America. Drawing irrigation water primarily from the High Plains (Ogallala) Aquifer, farmers in this area (approximately 200 x 250 km) use over 6×10^9 m^3 of irrigation water annually [*Ryder*, 1996]. This corresponds to an estimated 40cm/year of additional water, nearly doubling the surface water budget. Such a massive introduction of water to the surface can dramatically cool the surface and raise the latent heat flux as well as the convective available potential energy (CAPE). Almost all surface water in the Texas High Plains is injected into the lower atmosphere, not to groundwater or runoff [Reed, S., D. Maidment, & J. Patoux, "Spatial Water Balance of Texas," *CRWR Online Report 97-1,* 1997, at http://www.crwr.utexas.edu /gis/gishyd98/library/wbtexas/wbtexas.htm]. Recharge for the aquifer in the Southern High Plains is only 0.06cm per year, about 0.1 percent of annual precipitation [*Ryder*, 1996]. Although the irrigation water itself is not the primary source of precipitation, the surface moisture elevates the latent heat flux. A deeper layer of high equivalent potential temperature is formed which increases the gradient of moist static energy. This steeper gradient encourages deep convection, making precipitation more probable [*Eltahir,* 1998]. Hence the irrigation water represents an enormous perturbation of the regional atmospheric water and heat balance whose influence does not add significant moisture directly to storms but makes conditions more favorable for rainfall.

The Texas panhandle of the High Plains is an excellent area for the study of the influence of irrigation on climate and this is the region where we focus our analysis. In this region, irrigation is intense, topographic changes are minor and high-resolution radar-based precipitation measurements have been made since 1995.

Here we examine precipitation patterns in the summer months of 1996 and 1997. We chose these years because of the high contrast in precipitation magnitude – 1996 was a drought year and 1997 was a year of average precipitation – and because of the continuity of land use and irrigation patterns over those two years. If any change in precipitation is attributable to irrigation, the effects should be most evident during a relatively dry growing season and when the crop's demand for water is highest. Consequently, we expected to see the strongest evidence for an irrigation effect during the later part of the growing season in 1996.

2.Methods

A two-step procedure was employed to measure an irrigation effect: precipitation anomalies were identified using autocorrelation analysis, whereas the magnitude of effect was calculated using data from 19 rain gauge stations. Hourly precipitation data were collected for 2 summer seasons (June-August 1996 and June-August 1997) using Stage III WSR-88D Nexrad bias-corrected radar estimates from the NOAA Arkansas-Red Basin River Forecast Center (ABRFC) website (http://www.srh.noaa.gov/abrfc/). 6336 individual storm

events were identified over the two summer seasons and

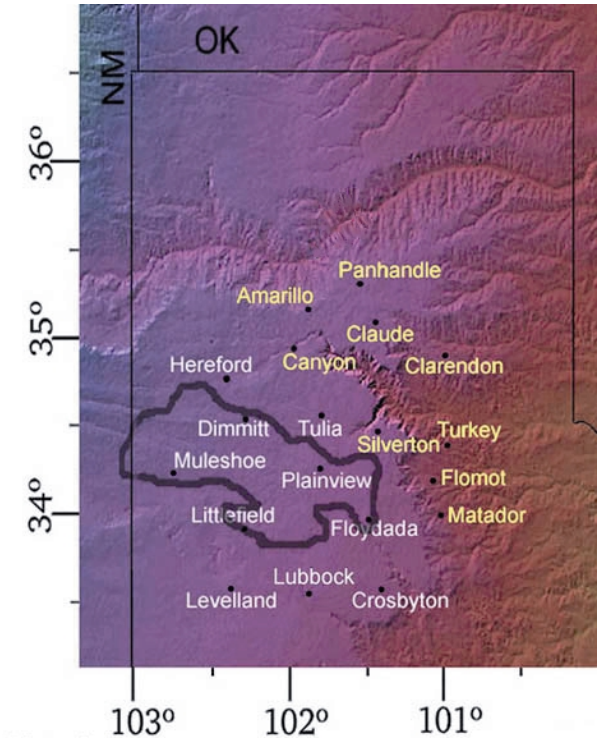

Plate 1. Texas High Plains study area including the 19 rain gauge stations used in this analysis. The intensively irrigated region (identified from Landsat images) is outlined in black. Stations in white lie in the irrigated area, including areas where irrigation is significant but scattered. Stations in yellow lie in the anomaly area; the unirrigated Amarillo and Panhandle stations fall just outside the 2σ contour but were included for completeness. Their inclusion has negligible effect on the analysis.

used to identify spatial anomalies by comparison of intensities, spatial lengths, temporal variability, and spatial orientation. A "storm event" means a single cohesive and isolated area within an image (e.g. one of several scattered thunderstorms) where rainfall is measured; several storm events often occur in the same image of hourly data.

Each hourly image was examined for storms within the boundaries of 100.0ºW to 103.5ºW and 33.0ºN to 36.5ºN. 1443 hourly images were used in this study (each image often contained several storm events); 17 were omitted, primarily due to poor image quality. Errors from the WSR-88D Stage III merging procedure depend on gauge density and are range-dependent; however, gauge density over this portion of the ABRFC collection area is remarkably uniform, and no trends or biases consistent with variations in gauge density were evident. Biases towards light precipitation (e.g. Pereira Fo. et al. [1998]) would primarily affect accumulation, not storm size, and should have only minimal influence on our results.

We used a two-dimensional autocorrelation function as a basic tool to compare the various precipitation events ("storm cells") in each image. This proved to be a better tool than PCA because it allowed for comparison among different storm events rather than integrating all storm events together for a given month. We calculate the autocorrelation function as

$$A_{k,j} = \frac{1}{(N-k)(M-j)} \sum_n \sum_m p_{n,m} p_{n+k,m+j}$$

Where N and M are the dimensions of the entire storm cell, and p is precipitation. Values of k extend to include negative offsets so that the autocorrelation function (almost always elliptical) is calculated for positive and negative vertical offsets and positive horizontal offsets; the $A_{k,j}$ ellipse points for the remainder of the domain (those with negative horizontal offset) were calculated by symmetry.

Following convention, we calculated an autocorrelation length (equal to $1/e$) from the semi-major axis of the ellipse, which served as a measure of storm coherence and size [*Bendat and Piersol,* 1986]. Each hourly image usually had several storm cells in it, each of which was processed to determine the autocorrelation function. The geographic center of each ellipse was positioned on the original storm cell's effective center, using an intensity- and distance-weighted average. In this way we were able to assign each autocorrelation ellipse a position on a regional map. These ellipses were cumulatively plotted to exhibit the differences in autocorrelation length from one area to another. In addition to autocorrelation lengths, we determined the maximum intensities, angular orientations (due East = 0º), and lengths of the semi-minor axes of all storm cells' autocorrelation functions.

To examine time variability, we constructed aggregate plots of the ellipses over 7 time periods: the 1st half (June to mid-July) and the 2nd half (mid-July to August) of the 1996 growing season, the 1st half and 2nd half of the 1997 growing season; the entire growing season of 1996, the entire growing season of 1997, and both growing seasons of 1996 and 1997 combined Each half-season had 28 precipitation sequences, defined in this study as any sequence of hourly measured rainfall with no gap in precipitation greater than 4 hours. As soon as 5 hours with no precipitation had elapsed, a new sequence was considered to have begun. "Mid-July" thus indicates the time by which half of all summer storms had occurred, not a specific date.

To determine the magnitude of the hypothesized irrigation effect, precipitation data for 11 summers gathered from NOAA's National Climate Data Center were used to compare rainfall accumulations in irrigated areas and in potential irrigation influenced areas, which were defined by larger-than average storm autocorrelation lengths.

Autocorrelation functions are dimensionless and describe properties of the entire region surrounding the storm cell investigated; they do not represent specific points in space. However, each ellipse *does* apply to the locale for which the function was calculated (the small

NxM box typically 20km x 20km surrounding each storm cell) and hence can be displayed as a location on a map to illustrate broader trends in storm autocorrelation lengths. Due to resolution limitations of 2 km on the available data, we excluded storms smaller than 6 km in length. These were not common, and their impact on the total rainfall in the region is negligible.

In order to compare the spatial extent of the irrigated area with the anomaly (irrigation effect) area (defined as the area where the cumulative autocorrelation lengths exceed 2σ -- 2 standard deviations), we spatially cross-correlated the extent of the irrigated area with the spatial distributions of semi-major axis lengths. This was expected to detect if the geometry of storms are altered by the size and shape of an irrigated area. Finally, we examined the spectrum of autocorrelation lengths in order to identify a dominant characteristic length (if any) that might result from the irrigation-induced surplus of rainfall over the anomaly area.

3. Results & Discussion

As noted above, the precipitation patterns for each year were significantly different. While 1996 was a year associated with a relatively severe drought in most of Texas, the Texas High Plains mostly was spared. Most of the precipitation fell in July and August during prime growing season. The spring was very dry and crops required irrigation very early in the growing season, leaving the surrounding unirrigated areas parched. The contrast between surface conditions in irrigated and unirrigated regions was very pronounced for most of that summer.

The 1997 growing season for the Texas High Plains saw more precipitation – nearly 15cm more than 1996 – and it was more evenly distributed through the summer. July and August 1997 received about 4 cm of accumulation less than July and August 1996, but the soil moisture and albedo contrasts between cultivated land and rangeland were much less distinct than in 1996.

Plate 2 shows cumulative lengths of the autocorrelation ellipses summed for the time periods given. The scale is dimensionless and represents the number of ellipses overlapping at a given point. Persistent in every time period, a region of higher rainfall (above the 2σ contour in Plate 2) is depicted very near to and downwind of the irrigated area.

In all cases, longer cumulative autocorrelation lengths can be found downwind of the irrigated region. The autocorrelation maps display the autocorrelation structure

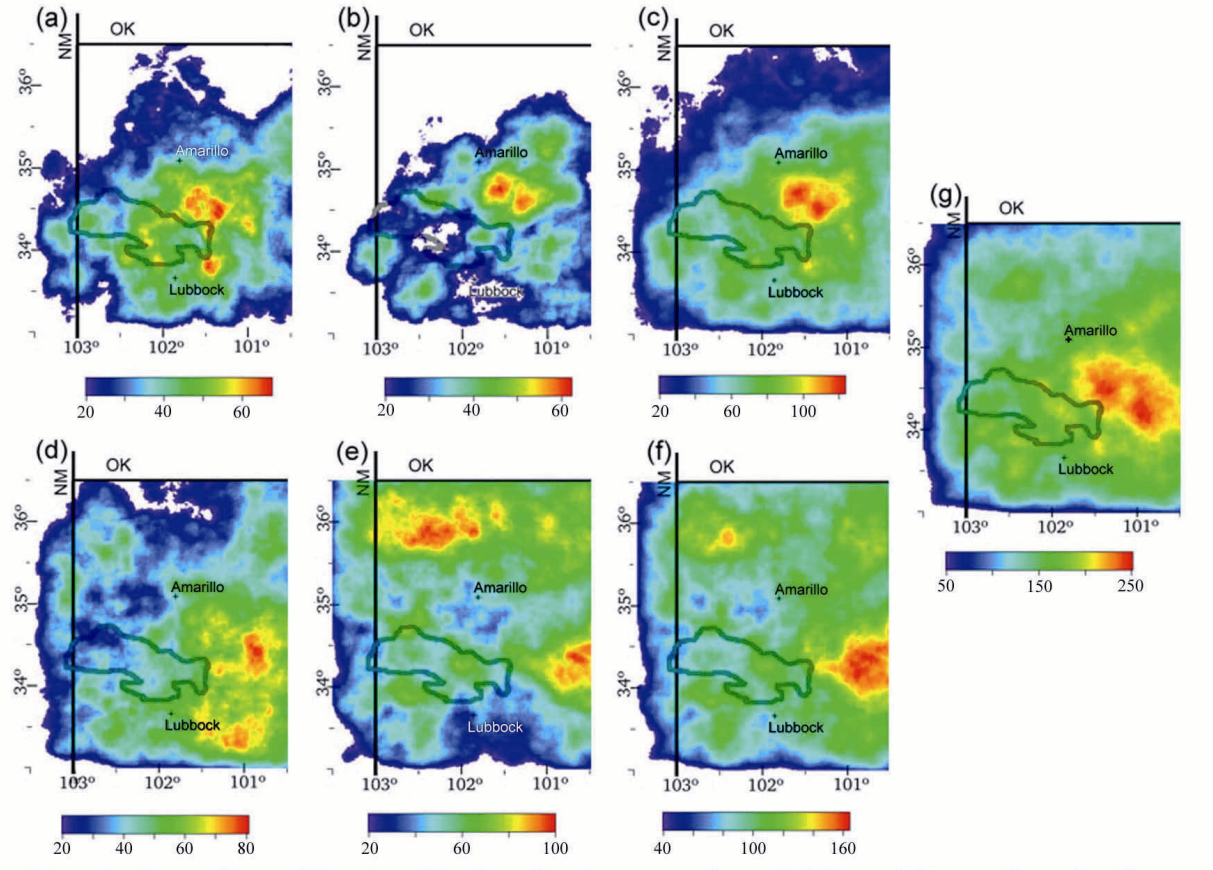

Plate 2. Cumulative autocorrelation lengths for seven time divisions. (a) June to mid-July 1996; (b) mid-July to August 1996; (c) June through August 1996; (d) June to mid-July 1997; (e) mid-July to August 1997; (f) June through August 1997; (g) sum of all 6 months. The 2σ contour is denoted by the warmer colors.

of regional storms relative to one another spatially. This proved to be a useful way to view the broad, general differences in autocorrelation lengths for storms over the irrigated area and over drier areas. In general, larger storms (e.g. mesoscale convective complexes) have longer duration and greater intensity. Prevailing summer surface winds are southerly and the prevailing winds at the 700mb level (where convective storms move) are west-south-westerly during the summer months for both years. Upper-air wind data can be obtained from the National Center for Atmospheric Research DSS archives. Edge effects of processing are visible but are distant and have no impact on the results.

Temporal differences are obvious from 1996 to 1997, and also between the 1st halves and 2nd halves of each year; even using different scales for all 7 time divisions, 1997 precipitation levels far surpass 1996 levels for each division. In the northernmost section of the Texas panhandle, precipitation in 1996 was very low, with precipitation below 40cm for the entire summer. The 2nd half of the 1997 summer season witnessed anomalously large autocorrelation lengths in this same northern section, which we attribute to natural variability.

Suppression over the irrigated area is very slight and not evident in any figures except 2(b), a result that essentially concurs with cloud formation studies [*e.g. Rabin et al.*, 1990]. As noted above, contrasts in surface temperature, humidity and CAPE between irrigated and dry regions were much greater in 1996 than in 1997; the autocorrelation maps for 1996 thus show more pronounced contrasts in rainfall.

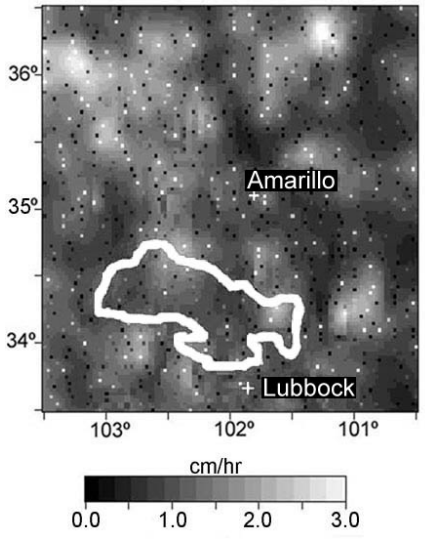

Figure 3. Spatial variations in intensity (interpolated using kriging) for the study region, summed over June-August 1996 and June-August 1997. Slightly larger events are downwind of the irrigated area as well as in the far northwestern corner. The "snow" (isolated white and black pixels) is individual measurements of intensity from which the general trends were interpolated.

Spatial variations in intensity (interpolated using kriging) for the study region, exhibit no distinct trends (Fig. 3). If anything, they show slightly larger events slightly downwind of the irrigated area as well as in the far northwestern corner. Since there are no distinct trends in precipitation intensity, we infer that the autocorrelation map indicates storms downwind have greater size and are of longer duration.

How much additional precipitation is attributable to an irrigation effect? Precipitation data for 11 summers gathered from NOAA's National Climate Data Center (Table 1) were used to compare rainfall accumulations in irrigated areas and in potential irrigation influenced areas, which were defined by larger-than average storm autocorrelation lengths.

Of 19 gauging stations in the region, 10 were within the "baseline" area on the flat Llano Estacado plateau (including 5 in the heavily irrigated area). These stations had an average summertime precipitation (June-August) that was exceeded by that of the anomaly (irrigation effect) area sites for 10 of the 11 years examined. Precipitation gauge sites in the anomaly area were selected if they were within the 189-level contour (above 2σ) of Plate 2(g). The average difference in precipitation for the eleven-year period is 3.8cm, with the anomaly area receiving roughly 18% surplus rainfall. This suggests that an irrigation effect is not strongly dependent on the degree of contrast in surface moisture between irrigated and unirrigated areas; rather, it is dependent on the existence of a contrast above some critical threshold. An average difference of 3.8cm, present for an entire decade, is not likely due solely to natural variability. Excluding the high value and the low value from the average, we still see an average surplus of 3.5cm (a 17% increase). The observed difference is significant at the level of $\alpha = 0.01$.

Topography is not responsible for the anomaly. Hills and valleys in the east (Plate 1) likely affect precipitation (the effect area is just east of the uniformly flat and featureless Llano Estacado). However, these hills and valleys span the entire study area from north to south.

There is a general east-west trend in precipitation (the north-south gradient is essentially zero) that likely explains some of the anomaly. Based on 30-year precipitation averages, the east-west precipitation gradient in this area is nearly linear and approximately 10cm per 300km. The center of the anomaly area is 75km east of the irrigated area's center. We can therefore attribute about 2.5cm of additional rainfall to this trend. The remainder, about 1.3cm (6% of summer precipitation), gives the lower bound for the irrigation effect.

We spatially cross-correlated the extent of irrigated area with the spatial distributions of semi-major axis lengths. This was expected to detect if the geometry of storms is altered by the size and shape of an irrigated area. Finally, we examined the spectrum of autocorrelation lengths in order to identify a dominant characteristic length (if any) that might result from the irrigation-induced surplus of rainfall over the anomaly area.

Cross-correlation of the cumulative autocorrelation length (Plate 2g) with the irrigated area produced a correlation distance of 90km. This offset distance was almost entirely along the east-west line, indicating that the irrigation effect influences storms at the 700mb level. This agrees with our hypothesis of sensible/latent heat flux balance governing the irrigation effect, with surface water providing little actual water to storms. At most, the equivalent of 3.8cm out of ~40cm applied via irrigation (10%) actually returns to the region.

A histogram of autocorrelation lengths is shown in Figure 4. Although the smallest storms were excluded from this study, more small storms were found over the irrigated area (black line) than over the anomaly area (gray line). Many more large storms were found over the anomaly area, indicating that storm duration was enhanced due to an irrigation effect. The average autocorrelation length for storms over the anomaly area was 24km, only slightly larger than the 20km average over the irrigated area.

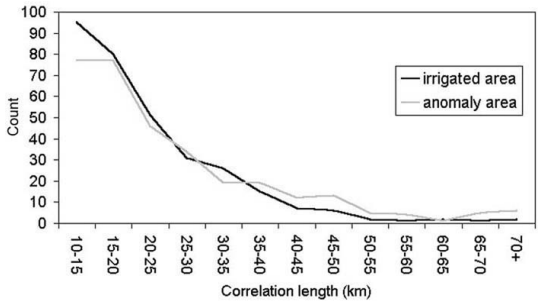

Figure 4. Histogram of storm autocorrelation lengths over irrigated and anomaly areas. Data are from June-August 1996 and June-August 1997. The difference in precipitation between the two areas generally increases with increased precipitation during the summer months (0.15 cm increase per cm of precipitation with $r^2 = 0.21$).

The Rossby deformation radius for this latitude is between approximately 90-120 km [*Pielke*, 2001]. Since mesoscale heat fluxes are most strongly influenced by spatial heterogeneities (wavelengths) approximating the Rossby radius [*Chen and Avissar*, 1994], the irrigation effect should be strongest when the near-surface wind direction is from the south-southwest, where the fetch of the irrigated region is about 100km. This is the predominant surface wind direction, and once mesoscale circulation starts, the perturbation will be carried to higher altitudes where storms can form.

4. Conclusion

We have shown that cumulative autocorrelation lengths downwind of a heavily irrigated area are longer, and that this perturbation of precipitation is due at least in part to intensive irrigation. No distinct spatial trends in precipitation intensity were observed, and irrigation did not significantly alter storm size or suppress rainfall directly above the irrigated area.

However, cumulative autocorrelation lengths were greater within an "anomaly area" about 90 km downwind of the irrigation area, indicating elongated storms, greater storm duration, or both. In comparing precipitation records for the irrigated and anomaly areas, we found that the irrigation effect accounted for 6% - 18% of downwind precipitation. The irrigation effect is so small that it is unlikely to be unequivocally identified using principal components analysis of monthly precipitation as was done in previous studies of the region [*Barnston and Schickedanz*, 1984; *Moore and Rojstaczer*, 2001].

Since intensity was unaffected by irrigation and the storms downwind were larger and delivered more accumulation, a portion of the additional rainfall may have come from the irrigated area itself. Irrigated agriculture is slowly pumping groundwater into the atmosphere, but an amount less than 10% of irrigation water applied is returned to the land surface in the region.

Models of specific thunderstorm events in the Texas High Plains [*Pielke et al*.,1997; *Ziegler et al*., 1997; *Weaver and Avissar*, 2001] suggest that there may exist a threshold amount of irrigation that will trigger the irrigation effect. Atmospheric conditions of the Texas High Plains instigate a negative moisture feedback directly overhead [*Findell*, 2001], but a supply of moisture and a cooler surface set the stage for the nearby dry, hot regions. Future research calls for a better understanding of what triggers these effects and of water cycling changes when human perturbations are involved.

Acknowledgments. This research was funded by the NASA Land Surface Hydrology Program.

References

Barnston, A. G. & P. T. Schickedanz, The effect of irrigation on warm season precipitation in the southern Great Plains. *J. Clim. Appl. Meteorol. 23*, 865-888, 1984.

Bendat, J. S. & A. G. Piersol, *Random Data: Analysis and Measurement Procedures*, ed. 2, Wiley, New York, 1986.

Chen, F. & R. Avissar, The impact of land-surface wetness heterogeneity on mesoscale heat fluxes. *J. Appl. Meteorol. 33*, 1323-1340, 1994.

De Ridder, K. & H. Gallée, Land surface-induced regional climate change in southern Israel. *J. Appl. Meteorol*., *37*, 1470-1485, 1998.

Eltahir, E. A. B. A Soil Moisture- Rainfall Feedback Mechanism, 1. Theory and Observations, *Water Resources Research 34*(4), 765-776, 1998.

Findell, K. Atmospheric controls on soil moisture-boundary layer interactions (thesis). MIT, Cambridge, Mass., 2001.

Fowler, W.B. & J. D. Helvey, Irrigation increases rainfall? (response) *Science, 188*, 281, 1975.

Lo, C. P., D. A. Quattrochi, & J. C. Luvall, Application of high-resolution thermal infrared remote sensing and GIS to access the urban heat island effect. *Int. J. Remote Sensing, 18*, 287-304, 1997.

Moore, N. & S. Rojstaczer, Irrigation-Induced Rainfall and the Great Plains. *J. Appl. Meteorol*., *40*, 1297-1309, 2001.

Pereira Fo., A.J., K.C. Crawford and C.L. Hartzell. 1998. Improving WSR-88D Hourly Rainfall Estimates. *Weather and Forecasting 13*: 1016-1028.

Pielke, R.A., T.J. Lee, J.H. Copeland, J.L. Eastman, C.L. Ziegler, & C.A. Finley, Use of USGS-provided data to improve weather and climate simulations *Ecol. Appl*., *7*, 3-21, 1997.

Pielke, R. A. Influence of the spatial distribution of vegetation and soils on the prediction of cumulus convective rainfall. *Reviews of Geophysics, 39*, 151, 2001.

Rabin, R. M., S. Stadler, P. J. Wetzel, D. J. Stensrud, & M. Gregory, Observed effects of landscape variability on convective clouds. *Bull. Am. Meteorol. Soc. 71*, 272-280, 1990.

Ryder, P. D. *Ground Water Atlas of the United States: Oklahoma, Texas. HA 730-E,* USGS, Washington, DC, 1996.

Stidd, C. K. Irrigation increases rainfall? *Science, 188*, 279-281, 1975.

Weaver, C. & R. Avissar, Atmospheric disturbances caused by human modification of the landscape. *Bull. Am. Met. Soc., 82*, 269-281, 2001.

Ziegler, C. L., T. J. Lee, & R. A. Pielke, Convective initiation at the dryline: A modeling study. *Mon. Wea. Rev. 125*, 1001-1026, 1997.

N. Moore and S. Rojstaczer, Center for Hydrologic Science, Division of Earth & Ocean Sciences, Duke University Box 90229, Durham, NC, 27708. (e-mail: njm@duke.edu or stuart@duke.edu)

Table 1. Summer precipitation at stations in the irrigated area and the anomaly area, 1987-1997.

irrigated			June+July+August precipitation (cm)										
Station Name	**Latitude**	**Longitude**	**1987**	**1988**	**1989**	**1990**	**1991**	**1992**	**1993**	**1994**	**1995**	**1996**	**1997**
Hereford	34.9733	102.6023	23.8	17.8	24.3	10.6	34.3	29.1	25.5	21.8	12.6	32.1	18.4
Plainview	34.0742	101.826	11.5	35.1	28.9	10.6	24.5	31.5	18	13.7	11.1	20.3	24.6
Dimmitt 2 N	34.5341	102.2567	18.6	17.3	30.3	12.8	29.2	33.8	22.9		22.9	22.6	28.1
Tulia	34.5295	101.7318	18.1	24.3	26.8	10.8	29.5	28.7	26.2	22	18.6	25.2	18.9
Muleshoe 1	34.0674	102.8297	22.5	18.9	21.8	9.8	22	21.6	18.9	17.9	12.5	31.5	24.4
Littlefield 2	34.0688	102.3475	22.3	18.1	29.3	10.8	16.6	22.4	19.1	11.7	6.2	42	20.5
Levelland	33.6058	102.3429	24.5	17	32	14	24.9	20.1	19.6	8.2	8.9	24.9	19.5
Crosbyton	33.6126	101.2975	29.6	10.5	20.2	14.2	29.2	24	22.9	6.4	14.4	25	19.4
Floydada	34.0737	101.303	15.9	25.6	32.3	13.3	25.7	26.6	12.2	10.2	20.9	32.7	24.6
Lubbock Airpt	33.6117	101.8198	21.3	12.4	21.1	12.7	24.6	19.5	16.2	7	13.7	24.3	18
		average:	20.8	19.7	26.7	12	26	25.7	20.1	13.2	14.2	28.1	21.6
		std dev:	5.1	7.1	4.6	1.6	4.9	5	4.3	6.1	5.2	6.5	3.5
anomaly													
Amarillo Airpt	35.3972	101.8947	18.8	26.8	30.6	15.8	15.1	31	27	21.9	19.7	36.2	25
Panhandle	35.4054	101.3548	26.3	18.9	29.9	12.1	26.7	37.4	30.3		29	39.6	22.3
Claude	34.9659	101.3527	28.2	25.3	34.7	10	23.4	27.2	28.6	21.8	25.8	37.1	20.7
Canyon	34.9684	101.9003	28.7	18.8	29.8	13.4	20.2	32.9	37.5	26.1	16.8	26.8	21.7
Clarendon	34.9622	100.8112	18.8	19.2	35.9	15.5	27.8	24.3	11.2	6.1	31.4	38.6	26.7
Flomot 2 NE	34.2666	100.9334	24.9	17.4	18.3	18	22	31.3	22	24	26.4	23.1	37.4
Matador	34.0616	100.8319	16.1	14	20.5	19.9	24	25.1	18.6	14	37.5	34.3	
Silverton	34.5256	101.2068	29.7	30.6	23.6	12.1	21.4	26.1	15.7	9	19.3	37.4	27.9
Turkey	34.3956	100.8972	27.4	28.8	26	11	28.5	35.2		8.36	33.9	41.7	
		average:	24.3	22.2	27.7	14.2	23.2	30.1	23.9	16.4	26.6	35	26
		std dev:	5.3	5.6	6.4	3.3	4	4.5	8.6	8.3	7	6	5.7
	Anomaly - irrigated:		3.5	2.5	1	2.2	-2.8	4.3	3.7	3.2	12.5	6.9	4.3
		% increase:	17	13	4	19	-11	17	19	24	88	25	20